

# Silicon carbonitride ceramics derived from polysilazanes

## Part II. Investigation of electrical properties

Christoph Haluschka<sup>1</sup>, Christine Engel, Ralf Riedel\*

*Technische Universität Darmstadt, Fachbereich Materialwissenschaft, Fachgebiet Disperse Feststoffe, Petersenstraße 23, D-64287 Darmstadt, Germany*

Received 10 March 1999; received in revised form 15 November 1999; accepted 29 December 1999

---

### Abstract

Electrical properties such as d.c.- and a.c.-conductivity, permittivity as well as thermopower of polysilazane-derived silicon carbonitride ceramics were studied depending on the pyrolysis conditions and subsequent annealing. The electrical properties were analysed to be extremely sensitive with respect to variations of the chemical composition, the solid state structure and the microstructure of the Si–C–N materials. Therefore, electrical investigations can be an important tool for the non-destructive characterisation of novel multicomponent carbide-nitride-based ceramics. In particular the d.c.-conductivity can be controlled within 15 orders of magnitude by (i) temperature, (ii) atmosphere and (iii) annealing time applied during synthesis. The main mechanism, which is proposed for the transport of charge carriers in the amorphous, highly disordered silicon carbonitride is the tunnelling of large polarons. In contrast, the electrical conductivity of the crystallised SiC/Si<sub>3</sub>N<sub>4</sub>-counterpart is dominated by the transport of electrons in the conduction band of nitrogen doped SiC particles. © 2000 Elsevier Science Ltd. All rights reserved.

**Keywords:** Electrical conductivity; Electrical properties; Impedance; Spectroscopy; Si–C–N; Thermopower

---

### 1. Introduction

Materials for electronic devices operating at high power and high frequencies as well as at high temperatures in harsh environments are of great fundamental and technological interest. One candidate material which meets the aforementioned requirements is crystalline silicon carbide (SiC). Amorphous, organosilicon polymer-derived and non-stoichiometric silicon carbonitride (SiCN) ceramics have also been shown to exhibit excellent high temperature structural properties such as oxidation and creep resistance.<sup>1–3</sup> However, only few data concerning the electrical characterisation of this novel class of materials are presently available. Electrical properties determined by d.c.-techniques were reported by Mocaer et al. for ceramic compacts derived from polycarbosilazanes.<sup>4</sup> Accordingly the hydrogenated silicon carbonitride showed a semiconducting

behavior, was thermally stable up to 1250°C and underwent crystallisation into  $\beta$ -SiC crystals surrounded by free carbon cage-like structures between 1250 and 1400°C. Finally, decomposition of the remaining Si–C–N phase giving additional  $\beta$ -SiC and free carbon takes place above 1400°C. The change of the microstructure correlates with the results of the d.c.-conductivity measurements which were carried out between room temperature and 400°C.

The electrical conductivity of polyhydrazinomethylsilane derived amorphous Si–C–N-ceramics was described by Scarlete et al.<sup>5</sup> The high d.c.-conductivity in the range of  $10^4$  ( $\Omega$  cm)<sup>–1</sup> has been reported to be caused by 4-fold co-ordinated nitrogen acting as donor.

Sawaguchi et al.<sup>6</sup> carried out d.c.- as well as a.c.-measurements up to 400°C and investigated the electrical properties of crystallised compacts which were obtained by hot-pressing of amorphous Si–C–N powders at 1800°C in the presence of sintering aids. In the same study, the influence of varying SiC volume fractions in the polycrystalline SiC/Si<sub>3</sub>N<sub>4</sub>-ceramics on the electrical behaviour is described. Nevertheless, the electrical conductivity of the amorphous Si–C–N-phase has not been reported.

---

\* Corresponding author. Fax: +49-61-5116-6346.

E-mail address: dg9b@tu-darmstadt.de (R. Riedel).

<sup>1</sup> Now with Robert Bosch GmbH, PF 10 60 50, D-70049 Stuttgart, Germany.

Here we present the d.c.- and a.c.- conductivity of amorphous Si–C–N-ceramics and polycrystalline SiC/Si<sub>3</sub>N<sub>4</sub> composites derived from a poly(hydridomethyl)silazane. It is evident that the electrical properties are controlled by the synthesis conditions, particularly by the pyrolysis atmosphere as well as by the annealing time and temperature and can be adjusted in a wide range. The measurements are correlated with the solid state reactions and phase transformations, which take place during synthesis as described in detail in Part I.<sup>7</sup> Furthermore, information on the mechanisms, which are responsible for the transport of charge carriers in the highly disordered amorphous materials and in the polycrystalline SiC/Si<sub>3</sub>N<sub>4</sub>-compacts can be derived. Since the transport mechanisms strongly depend on the temperature, the measurements were performed in the range between –170 and +800°C to allow a reliable interpretation of the obtained data.

## 2. Experimental procedure

The synthesis of the poly(hydridomethyl)silazane derived Si–C–N samples with the stoichiometry Si<sub>1.7</sub>C<sub>1.0</sub>N<sub>1.5</sub> was performed as described in Refs.<sup>7–9</sup> Traces of H and O were observed in the Si–C–N ceramics. Materials with reduced carbon content and carbon free samples were obtained by using Ar/NH<sub>3</sub> gas mixtures instead of pure Ar during the pyrolysis step.<sup>10</sup>

At temperatures above 1400°C, annealing in N<sub>2</sub> led to crystallisation and separation of micro-crystalline Si<sub>3</sub>N<sub>4</sub> and nano-crystalline SiC particles.<sup>7</sup>

The complex impedance (*Z*) of the materials investigated was determined in the frequency range between 20 Hz and 1 MHz by a 2 point technique using a fully automated autobalance bridge (HP 4284 A). The real and imaginary terms of *Z* were determined from the applied a.c.-voltage and the a.c.-current which flows through the sample. Silver suspension as contact layer was used for sufficient electrical contact between the sample and the measurement electrodes. Considering the geometry of the samples, the electrical conductivity and permittivity could be calculated.

## 3. Results and discussion

### 3.1. d.c.-Conductivity

In general, the investigated silicon carbonitride, Si<sub>1.7</sub>C<sub>1.0</sub>N<sub>1.5</sub>, shows semiconducting behaviour with a positive temperature coefficient of the electrical conductivity  $\sigma_{d.c.}$ . Plotted versus the reciprocal temperature, the electrical conductivity of the amorphous compacts exhibits a non-linear behaviour (Fig. 1), which is related to the high density of states within the “mobility gap”. In order to get information on the transport mechanism,  $\sigma_{d.c.}$  is plotted vs  $T^{-1/\gamma}$ . The electrical conductivity

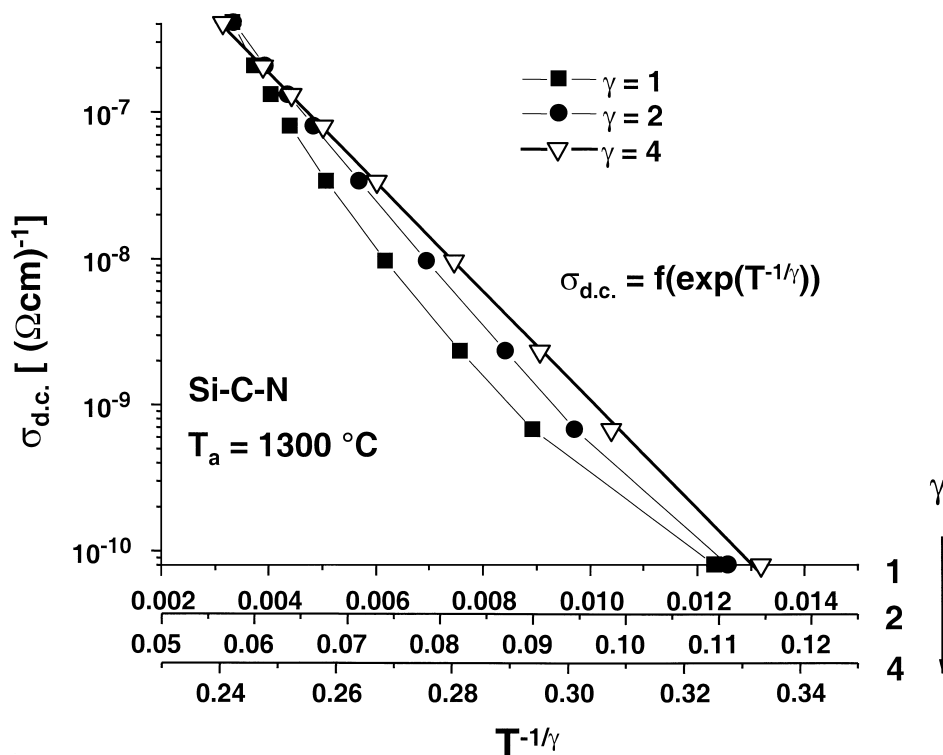


Fig. 1. Electrical conductivity  $\sigma_{d.c.}$  of amorphous silicon carbonitride ceramics depending on  $T^{-1/\gamma}$  with  $1 \leq \gamma \leq 4$ ;  $T_a$  = annealing temperature.

of the amorphous Si–C–N ceramic shows a linear behaviour for  $\gamma=4$  even at 130°C. Since single phonon assisted jumps of charge carriers is not valid for this temperature regime, a multi-phonon process is assumed to be responsible for the charge carrier transport.<sup>11</sup>

An increase of the d.c.-conductivity of about 8–10 orders of magnitude with increasing annealing temperature is measured (Fig. 2), whereas  $T_0$  which describes the temperature dependence of  $\sigma_{d.c.}$  according to Eq. (1), decreases (Fig. 3).

$$\sigma_{d.c.} \propto e^{-(T_0/T)^\gamma} \quad (1)$$

The electrical conductivity increase can be related to the main conducting phases developed during annealing. Therefore, three temperature regimes can be distinguished (Fig. 2) which correspond to the microstructural changes:<sup>7</sup>

In regime I ( $1000^\circ\text{C} < T_a < 1400^\circ\text{C}$ )  $\sigma_{d.c.}$  increases by as much as 3 orders of magnitude with growing annealing temperature. In addition to that,  $T_0$  decreases by one order of magnitude. This finding is attributed to a change of the solid state structure of the amorphous Si–C–N phase owing to the loss of residual hydrogen with increasing temperature. The H-content after pyrolysis at 1000°C is analysed to be about 5 at% and decreases during tempering.<sup>7</sup> The loss of hydrogen leads to an increase of the  $sp^2$ -/ $sp^3$ -ratio of the carbon atoms, which is proved by XANES-investigations at the CK-edge.<sup>7</sup> Consequently, the energy barrier for the transport of charge carriers is lowered and the electrical conductivity increases.

In regime II ( $T_a \geq 1400^\circ\text{C}$ ) a pronounced increase of the conductivity is observed in comparison to regime I. Note that the increase depends also on the isothermal annealing time  $t_a$ . For  $t_a = 25$  or 50 h, regime II starts at 1300°C.

According to TEM investigations the heat-treated samples contain microcrystalline  $Si_3N_4$ -grains with a carbon rich surface as well as nano-crystalline SiC with a particle size in the range of 2–5 nm.<sup>7</sup> The  $Si_3N_4$ -grains are isolated from each other. Therefore, the carbon rich surface does not contribute to the electrical conductivity. In contrast to this, the fraction of the SiC particles is about 16 vol%, which allows the formation of percolation paths throughout the sample.

Besides this, it was proved, that the nitrogen content of the remaining amorphous matrix decreases with growing annealing temperature, i.e. the chemical composition of the a-SiC(N) phase is more and more comparable to that of SiC.<sup>7</sup>

Consequently, the sharp increase of the electrical conductivity in regime II is attributed to both, the formation of nano-crystalline SiC and the reduction of the N-content in the amorphous matrix. However, it is still unclear, which of these effects dominates the conductivity.

At temperatures exceeding 1600°C (regime III) no  $sp^2$ -carbon can be detected by Raman spectroscopy.<sup>7</sup> The samples are completely crystalline and contain 40 wt%  $Si_3N_4$  and 60 wt% SiC as the conducting phase.

The measured conductivity of the composites annealed at 1700°C is about  $1 (\Omega \text{ cm})^{-1}$  at room temperature. This value is nearly the same as described by Kondo for recrystallised SiC.<sup>12</sup>

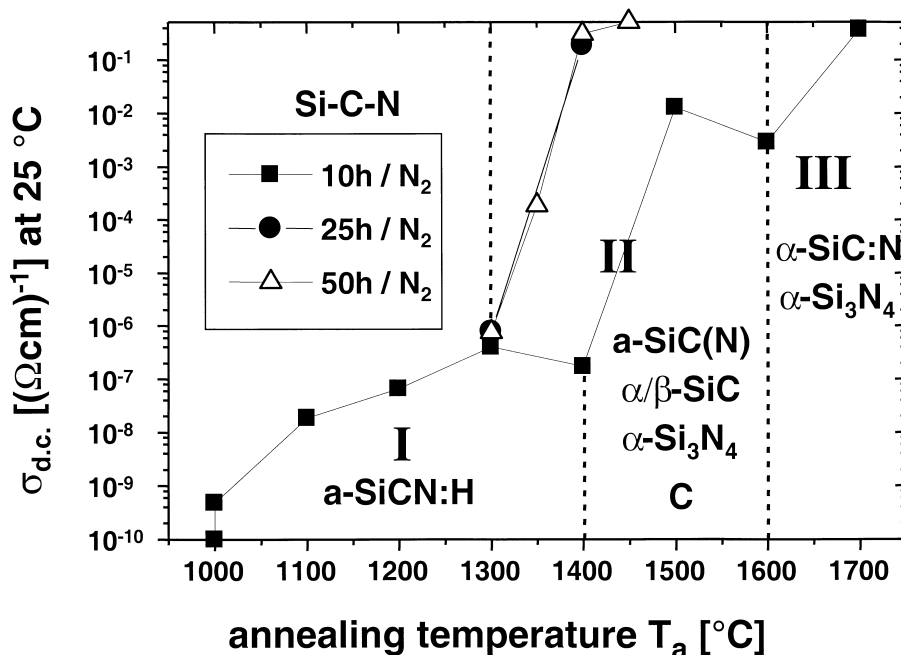


Fig. 2. Electrical conductivity  $\sigma_{d.c.}$  of amorphous silicon carbonitride ceramics depending on the annealing time  $t_a$  and the annealing temperature  $T_a$ .

The temperature dependence of the electrical conductivity is different to samples annealed in regime II, which also points out that no amorphous phase contributes to the conductivity.  $\sigma_{\text{d.c.}} \cdot T^{3/2}$  plotted against  $T^{-1}$  (Fig. 4) shows a linear behaviour in the temperature range between room temperature and 200°C according to Eq. (2):<sup>12</sup>

$$\sigma_{\text{d.c.}} \propto T^{-3/2} \exp\left(\frac{-E_{\text{d}}}{kT}\right) \quad (2)$$

From the gradient, the donor level  $E_{\text{d}} = 0.067$  eV  $\pm 1\%$  referred to the conduction band edge is derived corresponding to the dissolution of nitrogen in solid SiC. The  $n$ -doping of the silicon carbide is also proved by the determination of the thermopower  $S$ , which is in the range of  $10 \mu\text{V K}^{-1}$  measured at room temperature.

Above 400°C the conductivity reveals a higher slope in the Arrhenius plot (Fig. 4), which is caused by potential barriers present at the grain boundaries. In

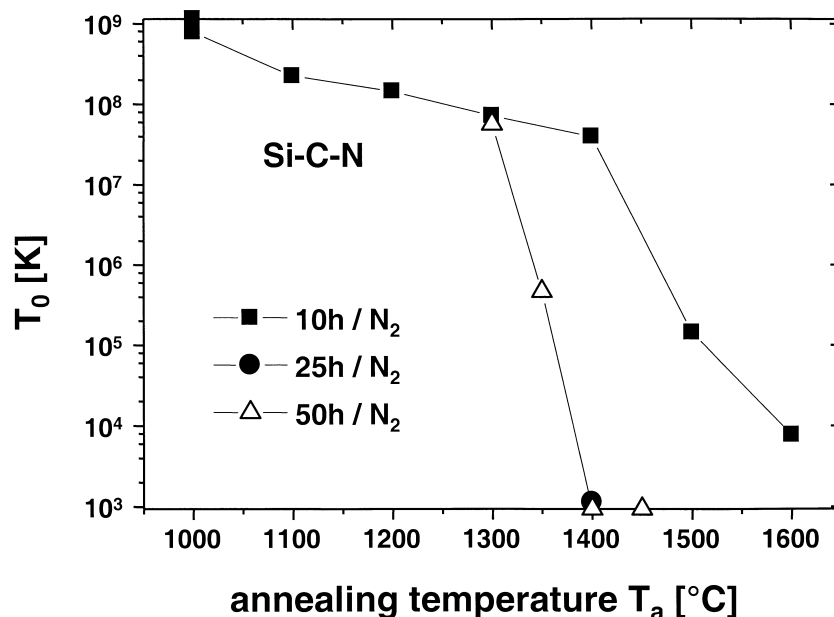


Fig. 3. Characteristic temperature  $T_0$  depending on the annealing time  $t_a$  and the annealing temperature  $T_a$ .

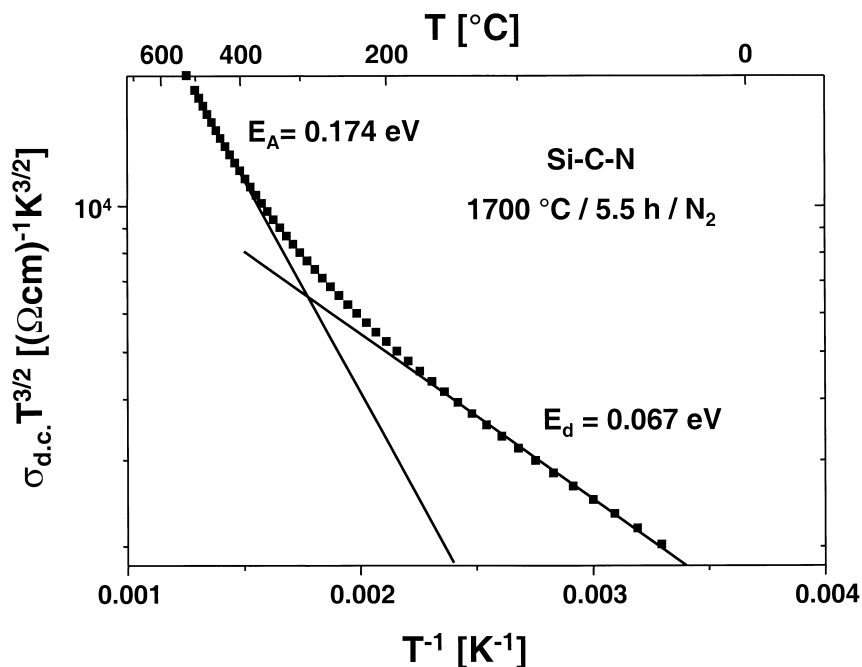


Fig. 4. Electrical conductivity  $\sigma_{\text{d.c.}}$  of a polycrystalline SiC/Si<sub>3</sub>N<sub>4</sub>-sample.

this temperature range the charge carriers cross the potential barriers by thermal activation (Fig. 5, case a), while at lower temperatures only tunnelling or hopping (Fig. 5, case b) has to be taken into account. This difference between low temperature and high temperature behaviour corresponds with a potential barrier height of about 0.1 eV, which is also consistent with that described for re-crystallised SiC.<sup>12</sup>

Apart from the annealing conditions, the pyrolysis atmosphere has a strong influence on the electrical properties. By using NH<sub>3</sub> or an Ar/NH<sub>3</sub>-mixture instead of pure Ar during the thermally induced ceramisation the carbon content of the ceramic product is reduced due to enhanced evolution of methane.<sup>7</sup> Accordingly, the C-content can be adjusted from about 14 wt% (Si<sub>1.7</sub>C<sub>1.0</sub>N<sub>1.5</sub>) to less than 0.5 wt% (Si<sub>3</sub>C<sub>x</sub>N<sub>4</sub> with  $x < 0.06$ ). With increasing substitution of carbon by nitrogen during pyrolysis in ammonia containing atmospheres, the stoichiometry resembles more and more that of silicon nitride. Therefore, the electrical conductivity is decreased by as much as 4 orders of magnitude (Fig. 6), i.e. the electrical properties are shifted from those of silicon carbonitride to those of silicon nitride. Consequently, engineering ceramics with a room temperature electrical conductivity ranging from 10<sup>-15</sup> to 1 (Ω cm)<sup>-1</sup> can be designed by the pyrolysis atmosphere and by the subsequent heat-treatment.

However, the temperature dependence of the conductivity  $T_0$  does not change under the influence of ammonia, indicating that the transport mechanism remains the same, i.e. the type of contributing states within the mobility-gap is unchanged.

### 3.2. a.c.-Conductivity

The temperature dependence of the d.c.-conductivity shows, that the transport mechanisms are dominated by

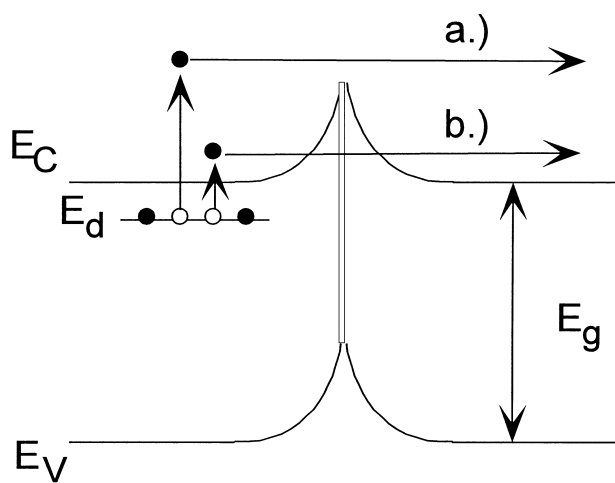


Fig. 5. Schematic of electrical transport across grain boundaries.<sup>7</sup> For (a) and (b) see text, Section 3.1.

electron states within the pseudo energy gap. Alternating current loss measurements are an important tool by which these deep defect centres can be studied,<sup>13</sup> since they are sensitive to processes in which such centres develop electronic dipole moments under the applied electrical field.

Fig. 7 shows the real part  $\sigma'$  of the conductivity depending on the annealing conditions. In accordance with a main feature of amorphous semiconductors the a.c.-conductivity increases with frequency  $\nu$  approximated by a power-law with the frequency exponent  $s \leq 1$ .<sup>14</sup>

$$\sigma(\nu) = A \cdot \nu^s \quad (3)$$

The origin of this behaviour is related to relaxation caused by hopping or tunnelling processes. Such relaxation processes are often described by using the pair approximation.<sup>13</sup> The alternating electrical field changes the environment of a pair of states and causes transitions between them. The resulting conductivity is dominated by pairs which have a relaxation time  $\tau$  of about  $\omega^{-1}$ . At high frequencies the a.c.-conductivity is originated by states which are separated by a small distance whereas at lower frequencies transitions over larger distances contribute to the a.c.-conductivity.

In the case  $\nu \rightarrow 0$  the conductivity is equal to  $\sigma_{d.c.}$ . As shown in Fig. 7, the d.c.-conductivity, which requires a continuous conducting path between the electrodes, becomes more important with increasing annealing temperature. After a heat-treatment at 1000°C the transition between pairs of states ( $\sigma'_{a.c.}$ ) still dominates the transport of charge carriers in the whole measured frequency range. In contrast, after annealing at 1300°C the d.c.-conductivity gives the main contribution to the overall electrical conductivity up to about 100 Hz. Samples heat-treated at 1500°C and higher show a frequency independent conductivity. This finding indicates that relaxation processes between single states do not cause any measurable contribution to the electrical conductivity dominated by percolation paths, exclusively.

Under the assumption that d.c.- and a.c.-conductivity do not effect each other,  $\sigma'$  can be expressed as:

$$\sigma'(\nu) = \sigma_{d.c.} + \sigma'_{a.c.}(\nu) \quad (4)$$

and the frequency exponent  $s$  becomes:

$$s = \frac{\nu}{\sigma'_{a.c.}(\nu)} \cdot \frac{\partial \sigma'_{a.c.}(\nu)}{\partial \nu} \quad (5)$$

By plotting  $s$  vs. the measuring temperature, the transport mechanism responsible for the a.c.-conductivity can be derived (Fig. 8).

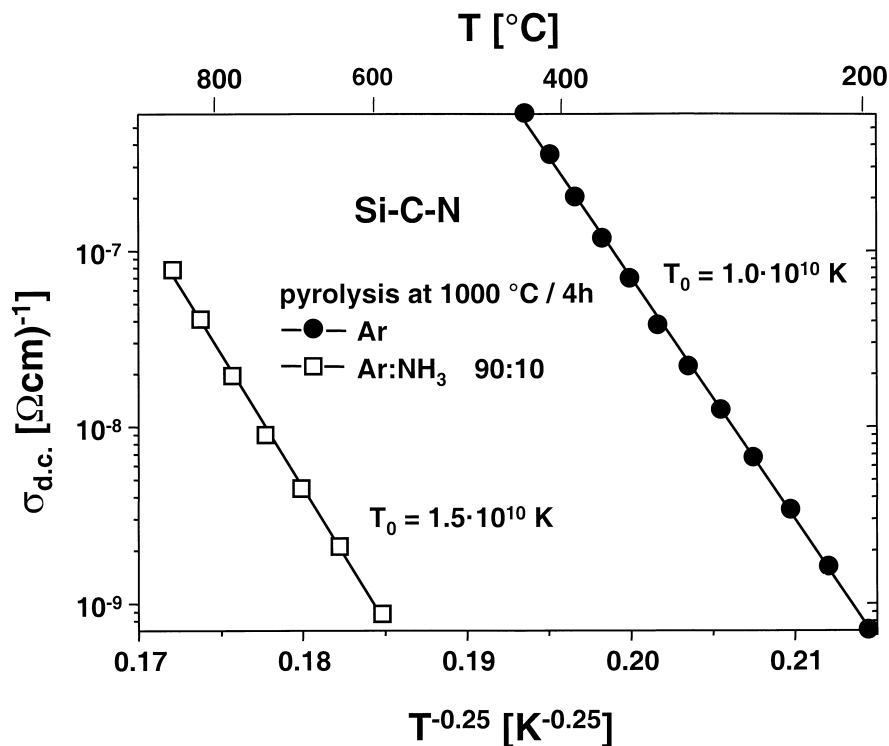


Fig. 6. Influence of the pyrolysis atmosphere on the temperature dependence of the electrical conductivity  $\sigma_{d.c.}$  vs.  $T^{-0.25}$ .

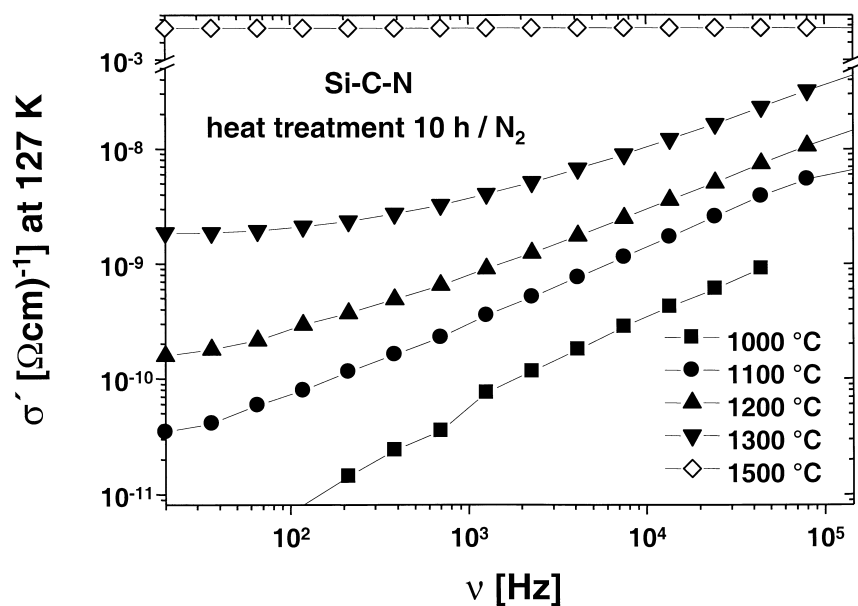


Fig. 7. Real part of the a.c.-conductivity  $\sigma'$  depending on the frequency  $\nu$  and the annealing temperature  $T_a$ .

The minimum of  $s(T)$ , which is a typical feature of large polaron tunnelling,<sup>13</sup> is shifted towards lower temperatures with increasing annealing temperature. Although the physical model of large polarons was developed for heteropolar ionic solids, this model can also be applied for

amorphous homopolar solids. This is due to a coulomb contribution to the interatomic forces caused by the lack of long-range order and by discontinuities associated with broken bonds and voids.<sup>13</sup> For the interpretation of the observed behaviour the Eqs. (6)–(8) are used:<sup>14</sup>

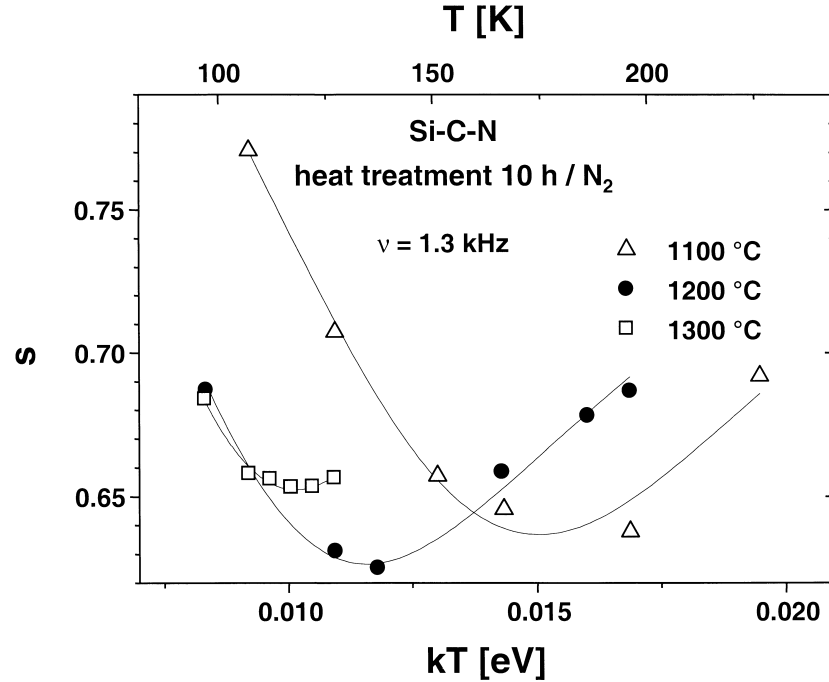


Fig. 8. Frequency exponent  $s$  depending on the measuring temperature  $T$  and the annealing temperature  $T_a$  (fitting curves are represented by lines).

$$s = 1 - \frac{6\alpha R_\omega + 6\beta W_{H0}r_0/R_\omega}{(2\alpha R_\omega + \beta W_{H0}r_0/R_\omega)^2} \quad (6)$$

with the fall-off of the wave function  $\alpha$ , the characteristic tunnelling distance  $R_\omega$  at a given frequency, the polaron radius  $r_0$  and  $\beta = 1/kT$ .  $R_\omega$  itself is a function of frequency and temperature and is described by

$$R_\omega = \frac{1}{4\alpha} \left[ -\ln(\omega\tau_0) - \beta W_{H0} + \sqrt{[-\ln(\omega\tau_0) - \beta W_{H0}]^2 + 8\alpha\beta r_0 W_{H0}} \right] \quad (7)$$

with a constant characteristic relaxation time  $\tau_0$  in the range of the inverse phonon frequency ( $10^{-13}$  s).<sup>13</sup> The parameter  $W_{H0}$  is related to the activation energy  $W_H$  corresponding to

$$W_H = W_{H0} \left(1 - \frac{r_0}{R}\right) \quad (8)$$

with the polaron separation  $R$ . According to Eqs (6)–(8), the parameters given in Table 1 were obtained by fitting the measured data of a sample tempered at 1300 °C in nitrogen.

It can be shown that the extension of the polaronic wave function  $\alpha^{-1}$  is about 1.3 times higher than the polaron radius  $r_0$  and according to Eq. (7) the tunnelling distance is 2.5 times higher than  $r_0$  (calculated for  $T = -170$  °C and  $\nu = 1.3$  kHz).

By using Eq. (9)

$$\sigma'_{a.c.}(\omega) = \frac{\pi^4}{12} e^2 (kT)^2 N^2(E_F) \frac{\omega R_\omega^4}{2\alpha kT + W_{H0}r_0/R_\omega^2} \quad (9)$$

the measured  $\sigma'_{a.c.}(\omega)$  data allow the determination of the normalised state density  $N(E_F)/\alpha^2$ , which at  $-170$  °C is in the range of  $10^6$  (eV cm)<sup>-1</sup>. The typical density of states  $N(E_F)$  in non-hydrogenated amorphous semiconductors is about  $10^{18}$  to  $10^{19}$ /eV cm<sup>3</sup>.<sup>13</sup> Taking into account, that only states within an energy range of about 0.01 eV around the Fermi level contribute to the conductivity at  $-170$  °C, it can be calculated, that the extension of the polaron wave function  $\alpha^{-1}$  is about 10 nm.

The temperature  $T_{min}$ , where the minimum of  $s(T)$  occurs, is characteristic for the activation energy  $W_{H0}$  according to the following estimation:<sup>13</sup>

$$T_{min} \approx 0.1 \cdot W_{H0}/k \quad (10)$$

Table 1  
Transport parameters of amorphous silicon carbonitride derived by fitting of the measured data

Fitting parameter	Range
$\alpha r_0$	0.7–0.8
$W_{H0}$ [eV]	0.2–0.4
$\tau_0$ [s]	$10^{-15}$ – $10^{-14}$

$T_{\min}$  and therefore  $W_{H0}$  decreases with increasing annealing temperature  $T_a$  (Fig. 8), indicating enhanced transfer of polarons. This is consistent with the increasing a.c.-conductivity with increasing annealing temperature.

In order to get more accurate data about the transport parameters depending on the heat treatment conditions, it is appropriate to interpret also the imaginary part of the conductivity  $\sigma''$  or the equivalent real part of the relative permittivity  $\epsilon'$ .

Plotting  $d\epsilon'/d\ln\nu$  vs the frequency  $\nu$  peaks were found within the curves (Fig. 9) which are typical for the relaxation processes in the tested material and are shifted to higher frequencies with increasing annealing temperature  $T_a$ . First it was Debye, who described such relaxation peaks by using only one characteristic relaxation time  $\tau_0$ .<sup>15</sup> In the case of amorphous materials, a single relaxation time cannot be assumed. Therefore, the parameter  $\alpha$  denoted as  $\alpha_{\text{Cole-Cole}}$  was introduced by Cole and Cole to consider a distribution of relaxation times,<sup>16</sup> which is symmetric around  $\tau_0$ . Moreover, asymmetric distributions were also proposed.<sup>17,18</sup>

In the symmetric case  $\epsilon'$  can be expressed as:

$$\epsilon' = \epsilon_\infty + (\epsilon_s - \epsilon_\infty) \frac{1 + (\omega\tau_0)^{(1-\alpha)} \sin(\alpha\pi/2)}{1 + 2(\omega\tau_0)^{(1-\alpha)} \sin(\alpha\pi/2) + (\omega\tau_0)^{2(1-\alpha)}} \quad (11)$$

with the static relative permittivity  $\epsilon_s$  ( $\omega \rightarrow 0$ ) and the relative permittivity  $\epsilon_\infty$  for high frequencies, at which the relaxation processes examined here do not contribute

to the polarisation. Deviating Eq. (11) and fitting the measured data leads to the following results (Table 2):

- The barrier height for polaron tunnelling  $W'$  which can be calculated from the slope of the relaxation frequency  $\nu_c$  (Fig. 10) according to Eq. (12)

$$\nu_c \propto e^{-\alpha R_0} \cdot e^{-W'/kT} \quad (12)$$

decreases with increasing  $T_a$ , which is consistent with the results obtained from  $s(T)$  (see Fig. 8).

- The parameter  $\alpha R_0$  ( $R_0$  is the maximum tunnelling distance) increases with growing  $T_a$ , i.e. polaron transfer across longer distances becomes more pronounced with increasing  $T_a$ .
- The parameter  $\alpha_{\text{Cole-Cole}}$  decreases with increasing  $T_a$ , i.e. the distribution of  $\tau_0$  which is influenced by the distribution of the separation distance  $R$  of the polarons becomes sharper.
- The relative permittivity  $\epsilon_\infty$  (high frequency limit) is in the range between 5 and 7 and nearly independent from  $T_a$ .

Table 2

Dielectric behaviour of amorphous silicon carbonitride depending on the annealing conditions

$T_a$ [°C]	$W'$ [meV]	$\alpha R_0$	$\alpha_{\text{Cole-Cole}}$	$\epsilon_\infty^a$
1100	$440 \pm 20$	3	$0.55 \pm 0.02$	$5.2 \pm 0.4$
1200	$160 \pm 10$	7	$\approx 0.30-0.40$	$6.0 \pm 0.4$
1300	$120 \pm 5$	7	$0.40 \pm 0.06$	$6.6 \pm 0.4$

<sup>a</sup> The  $\epsilon_\infty$ -values are corrected for porosity.

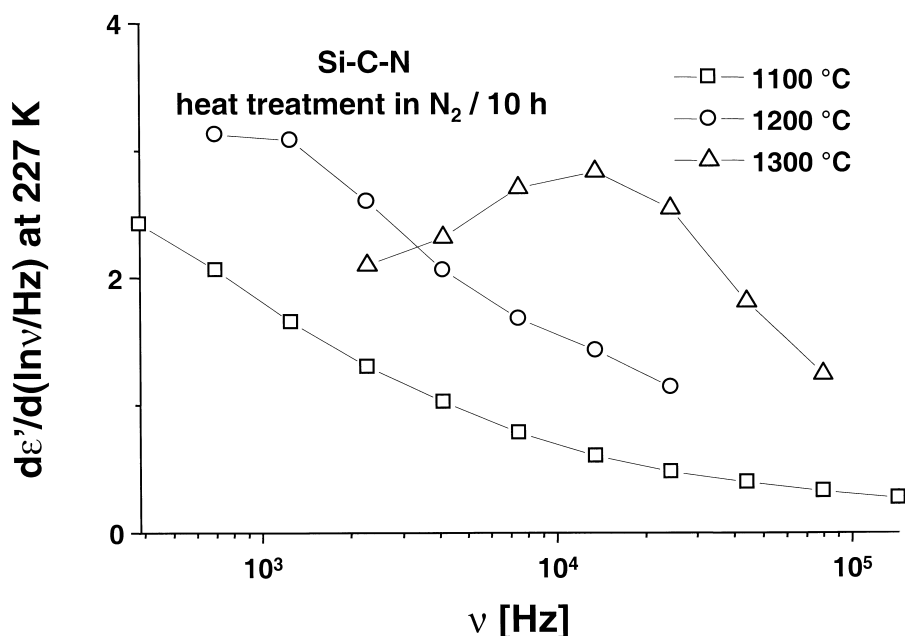


Fig. 9. Relaxation of the permittivity ( $d\epsilon'/d\ln\nu$  vs.  $\nu$ ) depending on the annealing temperature  $T_a$ .



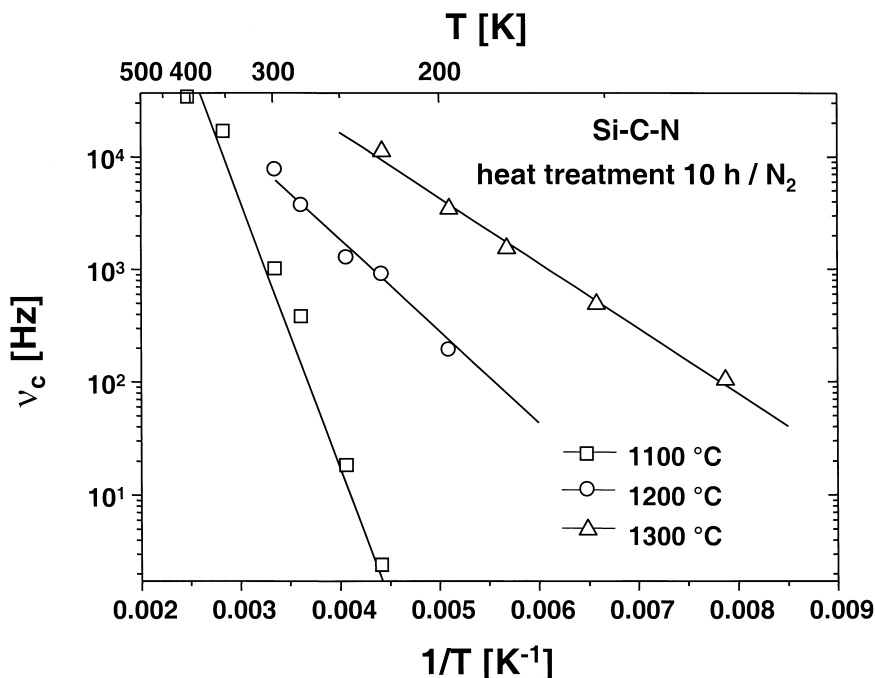


Fig. 10. Relaxation frequency  $\nu_c$  of Si-C-N ceramics depending on the measuring temperature  $T$  and the annealing temperature  $T_a$ .

The investigation of the a.c.-conductivity shows that the dielectric behaviour of these materials can be varied in a wide range by the synthesis conditions which can be of technological interest.

#### 4. Conclusion

The electrical properties of poly(hydridomethyl)-silazane-derived Si-C-N-ceramics can be summarised as follows:

(1) Silicon carbonitride shows a semiconducting behaviour with a  $T^{-1/4}$  dependence of  $\sigma_{d.c.}$  for the amorphous ceramics corresponding to transport within the band gap and a  $T^{-1}$  dependence for the polycrystalline  $\text{Si}_3\text{N}_4/\text{SiC}$  composite caused by transport in the conduction band. In the latter, the electrical conductivity is determined by the grain boundaries.

(2) The d.c.-conductivity is influenced by the conditions of the final heat treatment. Depending on the annealing temperature  $T_a$  three regions can be distinguished: (a) Increase of the conductivity of the amorphous SiCN matrix up to 1300°C caused by an enhanced  $\text{sp}^2/\text{sp}^3$ -ratio of the carbon atoms, (b) a strong increase of the conductivity due to the formation of SiC and the loss of nitrogen of the remaining amorphous a-SiC(N) matrix between 1300 and 1600°C and (c) the final electrical conductivity of nitrogen doped  $\beta$ -SiC above 1600°C which is proved by measurements of the thermopower. These findings are consistent with the

results obtained by  $^{15}\text{N}$ -method, XANES-spectroscopy, TEM, Raman-spectroscopy and XRD.<sup>7</sup>

Besides this, the conductivity depends on the isothermal annealing time of the Si-C-N materials at  $T_a$  exceeding 1300°C.

(3) By using an argon/ammonia - gas mixture instead of pure argon during the thermally induced ceramisation,  $\sigma_{d.c.}$  can be lowered by 4 orders of magnitude due to the substitution of carbon by nitrogen. Accordingly,  $\sigma_{d.c.}$  can be varied within 15 orders of magnitude by the pyrolysis atmosphere and by the subsequent heat-treatment. In contrast to the absolute value of  $\sigma_{d.c.}$  the conduction mechanism does not change in the ammonia treated samples.

(4) According to impedance spectroscopic investigations, the tunnelling of large polarons turns out to be the main transport mechanism in the amorphous Si-C-N materials. The barrier height  $W'$  is found to decrease with increasing annealing temperature, which corresponds with the increase of the a.c.-conductivity. The observed relaxations can be described by a modified Debye model, which introduces a distribution of relaxation times  $\tau$  instead of one single relaxation time  $\tau_0$ . Due to the heat treatment this distribution is found to become more discrete.

The results described here show that the electrical properties of amorphous Si-C-N ceramics are in the range between the electrical properties of semi-conducting SiC and that of insulating  $\text{Si}_3\text{N}_4$ . This enables to synthesise a variety of materials for electrical and electronic

applications just by changing composition and structure of the amorphous silicon carbonitride ceramics.

### Acknowledgements

This study has been performed under the project Ri 510-5/1 “Elektronische Eigenschaften neuer amorpher und nanokristalliner Keramiken”, supported by the Deutsche Forschungsgemeinschaft, Bonn, Germany. R.R. gratefully acknowledges the financial support by the Fonds der Chemischen Industrie, Frankfurt, Germany.

### References

1. Riedel, R., Kleebe, H. J., Schönfelder, H. and Aldinger, F., Covalent micro/nano-resistant to high temperature oxidation. *Nature*, 1995, **374**, 526–528.
2. Riedel, R., Kienle, A., Dreßler, W., Ruwisch, L., Bill, J. and Aldinger, F., A silicoboron carbonitride ceramic stable to 2000°C. *Nature*, 1996, **382**, 796–798.
3. Riedel, R., From molecules to materials. *Naturwissenschaften*, 1995, **82**, 12–20.
4. Mocaer, D., Pailler, R., Naslain, R., Richard, C., Pillot, J. P., Dunogues, J., Gerardin, C., Taulelle, F. and Si–C–N ceramics with a high microstructural stability elaborated from the pyrolysis of new polycarbosilazane precursors, Part I: the organic/inorganic transition, *J. Mater. Sci.*, 1993, **28**, 2615–2631.
5. Scarlete, M., He, J., Harrod, J. F. and Butler, I. S., Poly(methylsilane) and poly(hydrazinomethylsilane) as precursors for silicon containing ceramics, in applications of organometallic chemistry in the preparation and processing of advanced materials. *NATO ASI Series E: Applied Sciences*, 1994, **297**, 125–140.
6. Sawaguchi, A., Toda, K. and Niihara, K., Mechanical and electrical properties of silicon nitride–silicon carbide nanocomposite material. *J. Am. Ceram. Soc.*, 1991, **74**(5), 1142–1144.
7. Haluschka, C., Kleebe, H.-J., Franke, R. and Riedel, R., Silicon carbonitride ceramics derived from polysilazanes: Part I. Investigation of compositional and structural properties. *J. Eur. Ceram. Soc.*, 2000, **20**(9), 1355–1364.
8. Riedel, R., Passing, G., Schönfelder, H. and Brook, R. J., Synthesis of dense silicon based ceramics at low temperatures. *Nature*, 1992, **355**, 714–716.
9. Mayer, J., Szabó, D.-V., Rühle, M., Seher, M. and Riedel, R., Polymer-derived Si-based bulk ceramics, Part II: microstructural characterization by electron spectroscopic imaging. *J. Eur. Ceram. Soc.*, 1995, **15**, 703–715.
10. Galusek, D., Reschke, S., Lencés, Z., Dreßler, W. and Riedel, R., In-situ carbon content adjustment in Si–C–N bulk ceramics prepared by pyrolytic conversion of polyhydridomethylsilazane. *J. Eur. Ceram. Soc.*, 1999, **19**, 1911–1921.
11. Emin, D., Phonon-assisted jump rate in noncrystalline solids. *Phys. Rev. Lett.*, 1974, **32**, 303–307.
12. Kondo, A., Electrical conduction mechanism in recrystallized SiC. *J. Ceram. Soc. Jap., Int Edition*, 1992, **100**, 1204–1208.
13. Long, A. R., Frequency-dependent loss in amorphous semiconductors. *Adv. Phys.*, 1982, **31**(5), 553–637.
14. Elliott, S. R., a.c. Conduction in amorphous chalcogenide pnictide semiconductors. *Adv. Phys.*, 1987, **36**(2), 135–218.
15. Macdonald, J. R., *Impedance Spectroscopy*. John Wiley & Sons, New York, Chichester, Brisbane, Toronto, Singapore, 1987.
16. Cole, K. S. and Cole, R. H., Dispersion and absorption in dielectrics: I. Alternating current characteristics. *J. Chem. Phys.*, 1941, **9**, 341–351.
17. Havriliak, S. and Negami, S., A complex plane analysis of  $\alpha$ -dispersions in some polymer systems. *J. Polymer Sci.*, 1966, **C14**, 99–117.
18. Davidson, D. W. and Cole, R. H., Dielectric relaxation in glycerol, and n-propanol. *J. Chem. Phys.*, 1951, **19**, 1484–1490.